Permeative Flows in Cholesteric Liquid Crystals

D. Marenduzzo,[1] E. Orlandini,[2] and J. M. Yeomans[1]

[1]*Department of Theoretical Physics, Oxford University, 1 Keble Road, Oxford OX1 3NP, United Kingdom*
[2]*INFM, Dipartimento di Fisica, Universita' di Padova, Via Marzolo 8, 35131 Padova, Italy*

(Received 27 November 2003; published 4 May 2004)

We use lattice Boltzmann simulations to solve the Beris-Edwards equations of motion for a cholesteric liquid crystal subjected to Poiseuille flow along the direction of the helical axis (permeative flow). The results allow us to clarify and extend the approximate analytic treatments currently available. We find that if the cholesteric helix is pinned at the boundaries there is an enormous viscosity increase. If, instead, the helix is free the velocity profile is flattened, but the viscosity is essentially unchanged. We highlight the importance of secondary flows, and, for higher flow velocities, we identify a flow-induced double twist structure in the director field—reminiscent of the texture characteristic of blue phases.

DOI: 10.1103/PhysRevLett.92.188301 PACS numbers: 83.80.Xz, 47.50.+d, 61.30.–v, 83.50.–v

Liquid crystals are fluids, typically comprising long thin molecules, where subtle energy—entropy balances can cause the molecules to align to form a variety of ordered states [1,2]. In nematic liquid crystals the molecules tend to align parallel giving a state with long-range orientational order. This is usefully described by the director field $\vec{n}$, the coarse-gained, average, molecular orientation. In a cholesteric or chiral nematic liquid crystal $\vec{n}$ has a natural twist deformation in the direction perpendicular to the molecules. Examples of cholesteric liquid crystals are DNA molecules in solution, colloidal suspensions of bacteriophages [3], and solutions of nematic mixtures such as *E*7 with chiral dopants.

Liquid crystals exhibit both an elastic and a viscous response to an external stress. Coupling between the director and the velocity fields—known as backflow—leads to strongly non-Newtonian flow behavior. A particularly striking example in cholesterics is *permeation*. When a cholesteric liquid crystal is subjected to an imposed flow in the direction of the helix axis, its viscosity can increase enormously (by a factor $\sim 10^5$) when the isotropic to cholesteric transition is reached [4–6].

An explanation of permeation was given in [4]. If the director orientation is fixed in space, due, for example, to anchoring at the wall, any flow along the helix must be linked with a rotation of the molecules. This leads to an energy dissipation far larger than that due to the usual molecular friction and hence a much enhanced viscosity.

Balancing the dissipation from the director rotation with the energy gained from the pressure gradient along the capillary, Helfrich argued that the usual parabolic velocity profile is replaced by pluglike flow, with a constant velocity across the capillary [4]. To satisfy no-slip boundary conditions, however, the velocity must fall to zero at the edges of the sample. de Gennes and Prost [1] argue that this occurs over a length scale $\sim p$ where p is the pitch of the helix. Rey has extended these ideas to linear and oscillatory shear [7]. These calculations all assume small forcing, so that the director field is not deformed by the helix. There is an interesting suggestion in an early paper by Prost *et al.* [8] that an increase in forcing might stabilize a modulation in the director field in a direction perpendicular to the flow.

There are few quantitative experiments on cholesteric rheology, mainly as it is hard to obtain single domain textures or a uniformly pinned helix [5,6,9]. Porter *et al.* showed firm evidence for a high cholesteric viscosity at low forcing [5]. This dropped to values close to those of a normal liquid crystal as the shear rate was increased.

Helfrich's explanation of permeation is widely accepted, but many questions remain. There is confusion in the literature about whether the director field must be pinned in some way to obtain a permeative flow. It is interesting to ask whether distortions in the director field, induced by the flow, alter the permeation. Does permeation persist beyond the regime of low forcing and what replaces it for larger forcing? Finally, how does the interplay between the width of the boundary layer and that of the channel affect the flow?

Given the importance of cholesterics in optical devices and biological DNA solutions and the ubiquity of permeative flow in the theory of layered liquid crystals such as cholesterics and smectics [10] it is useful to develop a robust numerical method for solving the equations of cholesteric hydrodynamics, thus allowing us to probe questions that cannot be answered analytically.

Therefore in this Letter we solve numerically the hydrodynamic equations of cholesterics and hence clarify some of the outstanding questions about permeation. A major conclusion is the importance of boundary conditions. If the helix is pinned at the boundaries, e.g., by wall irregularities, the apparent viscosity increases by orders of magnitude. If the boundaries are free, the velocity profile is flat, but the helical structure is free to drift along the flow direction and the viscosity is much smaller. As the velocity of the system is increased, shear forces induce a significant deformation of the initial helix. First the cholesteric layers are bent into chevrons. Then at

higher forcing a doubly twisted texture is formed, the initial deformation being accompanied by a flow-induced twist in the perpendicular direction.

We consider the formulation of liquid crystal hydrodynamics given by Beris and Edwards [11]. The equations of motion are written in terms of a tensor order parameter $\mathbf{Q}$, which is related to the direction of individual molecules, $\hat{n}$, by $Q_{\alpha\beta} = \langle \hat{n}_\alpha \hat{n}_\beta - \frac{1}{3}\delta_{\alpha\beta} \rangle$ where the angular brackets denote a coarse-grained average and the Greek indices label the Cartesian components of $\mathbf{Q}$. The tensor $\mathbf{Q}$ is traceless and symmetric. Its largest eigenvalue, $\frac{2}{3}q$, $0 < q < 1$, describes the magnitude of the order.

The equilibrium properties of the liquid crystal are described by a Landau–de Gennes free energy density $\mathcal{F}$. This comprises a bulk term (summation over repeated indices is implied hereafter),

$$\frac{A_0}{2}\left(1 - \frac{\gamma}{3}\right)Q_{\alpha\beta}^2 - \frac{A_0\gamma}{3}Q_{\alpha\beta}Q_{\beta\gamma}Q_{\gamma\alpha} + \frac{A_0\gamma}{4}(Q_{\alpha\beta}^2)^2, \tag{1}$$

and a distortion term, which for cholesterics is [1]

$$\frac{K}{2}\left[(\partial_\beta Q_{\alpha\beta})^2 + \left(\epsilon_{\alpha\zeta\delta}\partial_\zeta Q_{\delta\beta} + \frac{4\pi}{p}Q_{\alpha\beta}\right)^2\right], \tag{2}$$

where K is an elastic constant. The tensor $\epsilon_{\alpha\zeta\delta}$ is the Levi-Civita antisymmetric third-rank tensor, A_0 is a constant, and γ controls the magnitude of order. The anchoring of the director field on the boundary surfaces is ensured by adding a surface term proportional to $(Q_{\alpha\beta} - Q^0_{\alpha\beta})^2$, with $Q^0_{\alpha\beta}$ chosen in such a way that the director has the desired orientation at the boundaries.

The equation of motion for $\mathbf{Q}$ is [11]

$$(\partial_t + \vec{u}\cdot\boldsymbol{\nabla})\mathbf{Q} - \mathbf{S}(\mathbf{W}, \mathbf{Q}) = \Gamma\mathbf{H}, \tag{3}$$

where Γ is a collective rotational diffusion constant and

$$\mathbf{S}(\mathbf{W}, \mathbf{Q}) = (\xi\mathbf{D} + \boldsymbol{\Omega})(\mathbf{Q} + \mathbf{I}/3) + (\mathbf{Q} + \mathbf{I}/3)(\xi\mathbf{D} - \boldsymbol{\Omega}) - 2\xi(\mathbf{Q} + \mathbf{I}/3)\mathrm{Tr}(\mathbf{QW}), \tag{4}$$

where Tr denotes the tensorial trace, while $\mathbf{D} = (\mathbf{W} + \mathbf{W}^T)/2$ and $\boldsymbol{\Omega} = (\mathbf{W} - \mathbf{W}^T)/2$ are the symmetric part and the antisymmetric part, respectively, of the velocity gradient tensor $W_{\alpha\beta} = \partial_\beta u_\alpha$. The constant ξ depends on the molecular details of a given liquid crystal. The term on the right-hand side of Eq. (3) describes the relaxation of the order parameter towards the minimum of the free energy. The molecular field $\mathbf{H}$ is given by

$$\mathbf{H} = -\frac{\delta\mathcal{F}}{\delta\mathbf{Q}} + (\mathbf{I}/3)\,\mathrm{Tr}\frac{\delta\mathcal{F}}{\delta\mathbf{Q}}. \tag{5}$$

The three-dimensional fluid velocity, $\vec{u}$, obeys the continuity equation and the Navier-Stokes equation,

$$\rho(\partial_t + u_\beta\partial_\beta)u_\alpha = \partial_\beta(\Pi_{\alpha\beta}) + \eta\partial_\beta[\partial_\alpha u_\beta + \partial_\beta u_\alpha + (1 - 3\partial_\rho P_0)\partial_\gamma u_\gamma \delta_{\alpha\beta}], \tag{6}$$

where ρ is the fluid density and η is an isotropic viscosity. The stress tensor $\Pi_{\alpha\beta}$ is

$$\Pi_{\alpha\beta} = -P_0\delta_{\alpha\beta} + 2\xi\left(Q_{\alpha\beta} + \frac{1}{3}\delta_{\alpha\beta}\right)Q_{\gamma\epsilon}H_{\gamma\epsilon} - \xi H_{\alpha\gamma}\left(Q_{\gamma\beta} + \frac{1}{3}\delta_{\gamma\beta}\right) - \xi\left(Q_{\alpha\gamma} + \frac{1}{3}\delta_{\alpha\gamma}\right)H_{\gamma\beta} - \partial_\beta Q_{\gamma\nu}\frac{\delta\mathcal{F}}{\delta\partial_\alpha Q_{\gamma\nu}} + Q_{\alpha\gamma}H_{\gamma\beta} - H_{\alpha\gamma}Q_{\gamma\beta}. \tag{7}$$

P_0 is a constant in the simulations reported here.

The differential Eqs. (3) and (6) are coupled. The order parameter field affects the dynamics of the flow field through the stress tensor. This is the backflow coupling. To solve these equations we use a lattice Boltzmann algorithm [12,13].

We consider a cholesteric liquid crystal that is sandwiched between two plates a distance L apart along the z axis. The axis of the cholesteric helix lies in a direction parallel to the plates that we shall take as the y axis. The primary flow is also along y, and is imposed via a pressure gradient. In the steady state, however, there can be secondary flow so that the modeling must be three dimensional. This geometry is the one for which permeation is expected. The elastic constants and viscosities are taken to have typical values for a cholesteric, and we consider channel widths $L \sim \mu$m. Typically, a cholesteric pitch was discretized by 64 lattice points, while 10^6 iterations were performed. Other details of the parameters for each simulation are given in the figure captions. There are no-slip velocity boundaries on the walls.

The results in Fig. 1 aim to compare the cases where the director at the wall is pinned or free to rotate. Consider first the case where the director is free. As a benchmark we show in Fig. 1(a) results from simulations where the backflow, i.e., the effect of the director field on the flow field, is turned off. The flow profile is as expected the parabola of Poiseuille flow. The cholesteric helix drifts at a slightly ($\sim$10%) smaller velocity than the flow. It is slightly bent by the flow into a chevron structure.

The origin of the chevron pattern can be identified by considering Eq. (3). Focusing on the center of the channel, $\mathbf{S}$ is zero, and the term $\vec{u}\cdot\vec{\nabla}\mathbf{Q}$—typical of this flow mode, in which the director field is not constant along the flow direction—must be balanced by a drift of the layers, $\partial_t\mathbf{Q}$. However, because of the parabolic shape of the velocity field, these cannot cancel exactly, and it is necessary to allow for a nonzero molecular field, resulting in the observed bending. The dominant elastic deformations associated with this steady state solution are splay and bend. The director field also develops a small component

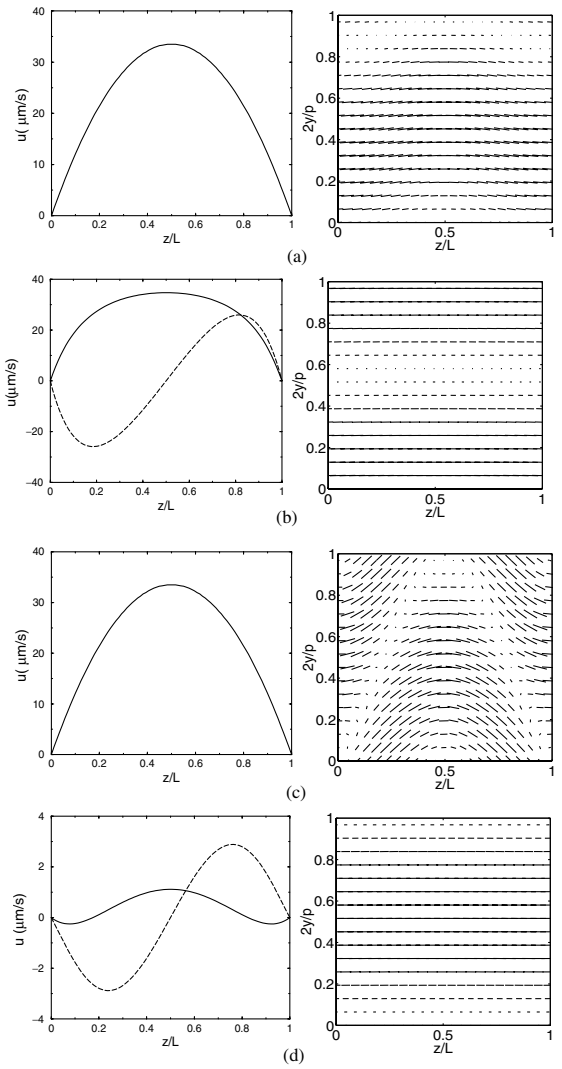

FIG. 1. Velocity (left) and director fields (right) for (a) free boundary conditions, no backflow; (b) free boundaries and backflow; (c) fixed boundaries, no backflow; (d) fixed boundaries and backflow. In (b) and (d) we also show the secondary flow (dashed line). This is an averaged velocity because the velocity field changes slightly along y due to the helical arrangement of the director field. The system studied corresponds to a cell of thickness $L = 2.25$ μm, and to a cholesteric with $p = 1.6$ μm, $K \sim 6.3$ pN. The rotational viscosity is $\gamma_1 = 1$ P, while the ratio between the Leslie viscosities α_2 and α_3 is $\alpha_3/\alpha_2 \sim -0.23$ (flow tumbling).

along the flow direction. This is caused by the shear forces contained in the tensor $\mathbf{S}$, which is nonzero away from the center of the channel.

Figure 1(b) compares the case when the full equations of motion, including backflow, are solved. The velocity is similar in magnitude, and the parabola flattens. This effect becomes more pronounced with an increase in L (Fig. 2). Our results are consistent with the picture described in [1] (although these authors consider pinned director boundary conditions) that the velocity profile

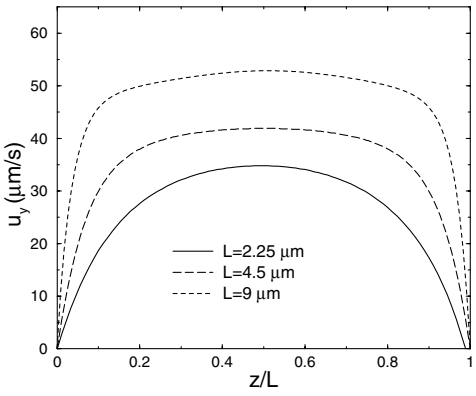

FIG. 2. Velocity profiles as a function of scaled distance along z. The pressure difference is scaled so that the velocity field of the liquid crystal in the isotropic phase is the same for all three sizes. The other parameters are as in Fig. 1.

in a wide system will be flat, decaying to zero near the boundaries in a length of order p to satisfy the no-slip conditions on the velocity. Also in this case the cholesteric helix drifts with the flow. A significant effect of the backflow is that there is much less bending of the helix, the pitch remaining constant across the system.

In the steady state we also find a secondary flow, of odd parity in z, along the x direction, which attains its maxima (in absolute value) close to the boundaries, and is zero in the center of the channel. The magnitude of this flow is comparable to the maximum fluid velocity along y, and it gives rise to shear forces that allow Eq. (3) to be balanced with a smaller director field deformation.

Now consider the case where the director is pinned at the wall (in such a way that there is no frustration in the helix when the system is at rest). Figure 1(c) shows the case without backflow. The velocity field is, as expected, identical to that in Fig. 1(a) because the director is having no effect on the flow. The helical texture is, however, much more deformed with a substantial component along y. This occurs because the director configuration is unable to drift with the flow, and thus the term $\vec{u} \cdot \vec{\nabla}\mathbf{Q}$ [in Eq. (3)] requires a larger balancing molecular field.

When backflow is turned on for this case there is a striking difference in the velocity profile. The net velocity is zero, to within the accuracy of the simulations (as would be expected from approximate analytic treatments [1,4]). Secondary flow is important: it is bigger than the maximum velocity attained in the primary flow. Because the velocities in the system are very small, the director field remains very close to its zero-flow configuration.

We now consider what happens as the pressure difference is increased. First, the chevrons gradually become more bent until a threshold forcing at which a new structure appears. This structure, shown in Fig. 3, has a flow-induced twist in the z direction. (The solution pictured in Fig. 1(c) corresponds to the threshold between the chevron and the double twisted texture.) The period of the

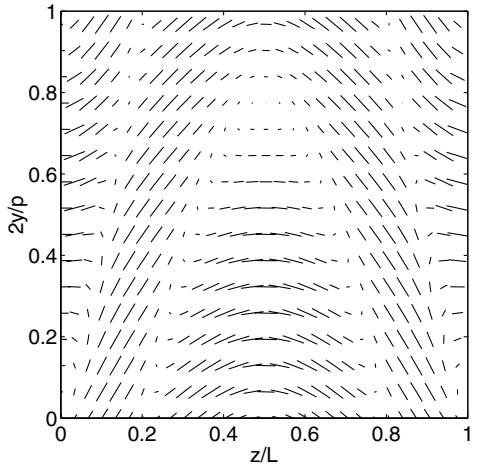

FIG. 3. Director field for a system with fixed boundary conditions. Parameters are $L = 3\ \mu$m, $p = 1.6\ \mu$m, $K \sim 6.3$ pN, $\alpha_3/\alpha_2 \sim 0.08$ (flow aligning). The maximum velocity in equilibrium is $\sim 45\ \mu\mathrm{m\,s^{-1}}$ (for $\gamma_1 = 1$ P). Note the double twist texture near the center of the channel.

twist along z is roughly equal to the natural twist of the cholesteric liquid crystal. This double twist structure was found for both flow-aligning (typically found in display devices) and flow tumbling (used in some rheological experiments [9]) viscosity regimes.

The maximum fluid velocity beyond which double twist appears depends sensitively on the system parameters. It is smaller if fixed boundary conditions are used. For example, for $K \sim 6$ pN, $L \sim 2.25\ \mu$m, $\alpha_3/\alpha_2 \sim -0.23$, and $p \sim 1.6\ \mu$m, with fixed boundary conditions the velocity threshold is $\sim 30\ \mu\mathrm{m\,s^{-1}}$ while for free boundaries it is an order of magnitude bigger. As L increases, the threshold velocity decreases if fixed boundaries are used. This effect is somewhat less pronounced with free boundaries. The crossover between chevrons and double twist is smooth; even at weak forcing one can identify a small twist deformation along z.

It is possible to explain qualitatively the appearance of a double twist via Eq. (3). Let us consider the case of anchored boundaries. Near the center of the channel, the solution is still determined by balancing the molecular field with $\vec{u} \cdot \vec{\nabla}\mathbf{Q}$, but since the flow is faster, the bending of the chevrons becomes more enhanced. When the deformation is such that two regions ordered along x are a distance $\sim p$ apart along the z axis, a doubly twisted state is expected to be more stable. Such a texture is reminiscent of the doubly twisted cylinders that are the basic constituents of blue phases [1]. Indeed, without backflow, where the simulations are stable for faster flows, a stack of such doubly twisted cylinders, separated by a regular array of defects, is stabilized by a large enough forcing.

Our results suggest that in real experiments [5,6,9], for slow flows, the helix is likely pinned to its initial configuration (e.g., by irregularities), so that the situation is close to that in Fig. 1(d) and the viscosity is very large. If the pressure difference is increased, either the pinning is destroyed or a double twist forms. In both cases the viscosity decreases as observed experimentally.

In conclusion, we have presented lattice Boltzmann simulations able to successfully simulate Poiseuille flow in cholesteric liquid crystals in the permeation mode. For weak forcing, if the cholesteric helix is pinned at the boundaries, we find a remarkable increase in the viscosity. With free boundaries there is a pluglike velocity profile in which the helix drifts with the flow. Beyond a threshold, dependent on system parameters, the flow distorts the helix much more, giving rise to a doubly twisted director pattern. This approach could be used to investigate, for the first time, the rheology of blue phases. Predictions can be tested with present day microchannel experiments. In particular, a fast Poiseuille flow may provide a novel method of inducing double twist in a liquid crystal texture, thus allowing controlled experiments on blue phases.

This work was supported by EPSRC Grant No. GR/R83712/01.

[1] P. G. de Gennes and J. Prost, *The Physics of Liquid Crystals* (Clarendon Press, Oxford, 1993), 2nd ed.
[2] S. Chandrasekhar, *Liquid Crystals* (Cambridge University Press, Cambridge, 1980).
[3] E. Grelet and S. Fraden, Phys. Rev. Lett. **90**, 198302 (2003).
[4] W. Helfrich, Phys. Rev. Lett. **23**, 372 (1969); T. C. Lubensky, Phys. Rev. A **6**, 452 (1972).
[5] R. S. Porter, E. M. Barrall II, and J. F. Johnson, J. Chem. Phys. **45**, 1452 (1966).
[6] N. Scaramuzza, F. Simoni, R. Bartolino, and G. Durand, Phys. Rev. Lett. **53**, 2246 (1984).
[7] A. D. Rey, J. Rheol. **46**, 225 (2002); **44**, 855 (2000); Phys. Rev. E **65**, 022701 (2002).
[8] J. Prost, Y. Pomeau, and E. Guyon, J. Phys. II (France) **1**, 289 (1991).
[9] K. Hongladarom, V. Secakusuma, and W. R. Burghardt, J. Rheol. **38**, 1505 (1994).
[10] See, e.g., A. N. Shalaginov, L. D. Hazelwood, and T. J. Sluckin, Phys. Rev. E **60**, 4199 (1999).
[11] A. N. Beris and B. J. Edwards, *Thermodynamics of Flowing Systems* (Oxford University Press, Oxford, 1994).
[12] C. Denniston, E. Orlandini, and J. M. Yeomans, Europhys. Lett. **52**, 481 (2000); Phys. Rev. E **63**, 056702 (2001); G. Toth, C. Denniston, and J. M. Yeomans, Comput. Phys. Commun. **147**, 7 (2002).
[13] C. Denniston, D. Marenduzzo, E. Orlandini, and J. M. Yeomans, cond-mat/0312123; J. Jung *et al.*, Liq. Cryst. **30**, 1455 (2003).